

Cyanide-Bridged Molecular Squares with Ferromagnetically Coupled  $d\pi$ ,  $d\sigma$ , and  $p\pi$  Spin SystemHiroki Oshio,\*<sup>†</sup> Masashi Yamamoto,<sup>‡</sup> and Tasuku Ito<sup>†</sup>

Departments of Chemistry, University of Tsukuba, Tennodai 1-1-1, Tsukuba 305-8571, Japan, and Graduate School of Science, Tohoku University, Aoba-ku, Sendai 980-8578, Japan

Received March 22, 2002

Cyanide-bridged molecular squares of  $[\text{Fe}^{\text{II}}_2\text{Cu}^{\text{II}}_2(\mu\text{-CN})_4(\text{dmbpy})_4(\text{impy})_2](\text{ClO}_4)_4 \cdot 4\text{CH}_3\text{OH} \cdot \text{C}_6\text{H}_6$  (**1**) and of  $[\text{Fe}^{\text{III}}_2\text{Cu}^{\text{II}}_2(\mu\text{-CN})_4(\text{dmbpy})_4(\text{impy})_2](\text{ClO}_4)_6 \cdot 4\text{CH}_3\text{OH} \cdot 4\text{H}_2\text{O}$  (**2**) (dmbpy = 4,4'-dimethyl-2,2'-bipyridine; impy = 2-(2-pyridyl)-4,4,5,5-tetramethyl-4,5-dihydro-1H-imidazolyl-1-oxy) were prepared. In the squares of **1** and **2**, the Fe(II/III) (low spin) and Cu(II) ions are alternately bridged by the cyanide groups, in which the cyanide carbon atoms coordinated to the Fe(II) ions and Cu(II) ions are coordinated by imino nitroxide. Magnetic susceptibility measurements for **1** and **2** revealed that the Cu(II) ion and imino nitroxide are ferromagnetically coupled with a fairly strong coupling constant ( $J_{\text{Cu-radical}} > 300$  K) and act as triplet species. In **1** the Cu(II)–radical moieties are magnetically separated by the Fe(II) ions. In the square of **2**,  $d\pi$  (Fe(III)),  $d\sigma$  (Cu(II)), and  $p\pi$  (imino nitroxide) spins are alternately assembled, and this situation allowed the square to have an  $S = 3$  spin ground state. The exchange coupling constant of Fe(III) and the Cu(II)–radical moiety in **2** was estimated to be  $J = 4.9 \text{ cm}^{-1}$  ( $H = -2\sum S_{\text{Fe}} \cdot S_{\text{Cu-radical}}$ ).

## Introduction

Considerable interest exists concerning molecule-based magnetic materials. Cyanometalates have been used to prepare infinite systems that behaves as high  $T_c$  magnets and photoinduced magnetic materials.<sup>1</sup> Due to the discovery of superparamagnetic behavior in dodecanuclear manganese clusters, efforts in the synthesis of multinuclear complexes with high-spin ground states have intensified and cyanometalates are of particular interest due to the bridging ability.<sup>2</sup> In other words, synthetic routes can be developed using cyanide-bridged bimetallic units to tune the nuclearity and spin multiplicity of complex molecules. A cyanide-bridged heptamer having one Mn(II) and six Cr(III) ions has an  $S =$

$13/2$  spin ground state due to the antiferromagnetic interactions,<sup>3</sup> while clusters having  $[\text{Mn}_9\text{W}_6]$  and  $[\text{Mn}_9\text{Mo}_6]$  cores have  $S = 39/2$  and  $51/2$  spin ground states, respectively.<sup>4</sup> Recently, it was shown that the introduction of organic radicals into cyanide-bridged clusters enhances the spin multiplicity of the clusters. Cyanide-bridged  $[\text{Fe}_2\text{Ni}_3]$  and  $[\text{Cr}_2\text{Ni}_3]$  clusters with imino nitroxides coordinated to the Ni ions have the spin ground state of  $S = 7$  and  $S = 9$ , respectively.<sup>5</sup> Recently, some cyanide-bridged molecular squares were reported by us and other groups, and we report that the squares of  $[\text{M}_2\text{M}'_2(\mu\text{-CN})_4(\text{bpy})_x]^{n+}$  ( $\text{M} = \text{Fe}$  and  $\text{M}' = \text{Fe}, \text{Co},$  or  $\text{Cu}$ ;  $x = 6$  or  $8$ ), abbreviated as  $[\text{M}_2\text{M}'_2]$ , have different electronic and magnetic properties depending on the metal ions and oxidation state.<sup>6</sup> The electrochemical two-electron oxidation of the diamagnetic  $[\text{Fe}^{\text{II}}_2\text{Fe}^{\text{II}}_2]$  gave

\* To whom correspondence should be addressed. E-mail: oshio@chem.tsukuba.ac.jp.

<sup>†</sup> University of Tsukuba.

<sup>‡</sup> Tohoku University.

- (1) (a) Ferlay, S.; Mallah, T.; Ouahès, R.; Veillet, P.; Verdaguer, M. *Nature* **1995**, *378*, 701. (b) Entley, W. R.; Girolami, G. S. *Science* **1995**, *268*, 397. (c) Sato, O.; Iyoda, T.; Fujishima, A.; Hashimoto, K. *Science* **1996**, *271*, 49. (d) Larionova, J.; Clérac, R.; Sanchiz, J.; Kahn, O.; Golhen, S.; Quahab, L. *J. Am. Chem. Soc.* **1998**, *120*, 13088.
- (2) (a) Henrich, J. L.; Berseth, P. A.; Long, J. R. *Chem. Commun.* **1998**, 1231. (b) Scuiller, A.; Mallah, T.; Verdaguer, M.; Nivorozhkin, A.; Tholence, J.-L.; Veillet, P. *New J. Chem.* **1996**, *20*, 1. (c) Vernier, N.; Bellessa, G.; Mallah, T.; Verdaguer, M. *Phys. Rev. B* **1997**, *56*, 75. (d) Klausmeyer, K. K.; Rauchfuss, T. B.; Willson, S. R. *Angew. Chem., Int. Ed.* **1998**, *37*, 1694.

- (3) Heinrich, J. L.; Sokol, J. J.; Hee, A. G.; Long, J. R. *J. Solid State Chem.* **2001**, *159*, 293.

- (4) (a) Zhong, G.; Seino, Z. J.; Mizobe, Y.; Hidai, M.; Fujishima, A.; Ohkoshi, S.; Hashimoto, K. *J. Am. Chem. Soc.* **2000**, *122*, 2952. (b) Larionova, J.; Gross, M.; Pilkington, M.; Andres, H.; Stoeckli-Evans, H.; Grüdel, H. U.; Decurtins, S. *Angew. Chem., Int. Ed.* **2000**, *39*, 1605.

- (5) (a) Marvilliers, A.; Pei, Y.; Boquera, J. C.; Vostrikova, K. E.; Paulsen, C.; Rivière, E.; Audière, J.-P.; Mallah, T. *Chem. Commun.* **1999**, 1951. (b) Marvilliers, A.; Hortholary, C.; Rogez, G.; Audière, J.-P.; Rivière, E.; Boqyeram, J. C.; Paulsen, C.; Villar, V.; Mallah, T. *J. Solid State Chem.* **2001**, *159*, 302. (c) Vostrikova, K. E.; Luneau, D.; Wernsdorfer, W.; Rey, P.; Verdaguer, M. *J. Am. Chem. Soc.* **2000**, *122*, 718.

the mixed-valent  $[\text{Fe}^{\text{II}}_2\text{Fe}^{\text{III}}_2]$  square with an  $H_{\text{ab}}$  value of 870  $\text{cm}^{-1}$ , and the mixed-metal square  $[\text{Fe}^{\text{III}}_2\text{Cu}^{\text{II}}_2]$  has an  $S = 2$  ground state. We report here a new class of cyanide-bridged  $[\text{Fe}_2\text{Cu}_2]$  high-spin squares with imino nitroxides on the Cu(II) ions.

## Experimental Section

**Materials.**  $[\text{Fe}^{\text{II}}(\text{CN})_2(\text{dmbpy})_2]$ ,<sup>7</sup>  $[\text{Fe}^{\text{III}}(\text{CN})_2(\text{dmbpy})_2](\text{NO}_3)$ ,<sup>8</sup> and imino nitroxide radical<sup>5</sup> ( $\text{dmbpy} = 4,4'$ -dimethyl-2,2'-bipyridine;  $\text{imp}y = 2$ -(2-pyridyl)-4,4,5,5-tetramethyl-4,5-dihydro-1H-imidazolyl-1-oxy) were prepared by the literature methods.

**Syntheses.**  $[\text{Fe}^{\text{II}}_2\text{Cu}^{\text{II}}_2(\mu\text{-CN})_4(\text{dmbpy})_4(\text{imp}y)_2](\text{ClO}_4)_4 \cdot 4\text{CH}_3\text{OH} \cdot \text{C}_6\text{H}_6$  (**1**),  $[\text{Fe}^{\text{II}}(\text{CN})_2(\text{dmbpy})_2]$  (106 mg, 0.2 mmol) in hot MeOH (30 mL) was added to a methanol solution (10 mL) of  $\text{Cu}(\text{ClO}_4)_2 \cdot 6\text{H}_2\text{O}$  and  $\text{imp}y$  (44 mg, 0.2 mmol). The mixture was heated to boil and concentrated to 15 mL, and then cooled to room temperature. Brown powder (135 mg) was collected by filtration, and recrystallization from methanol–benzene solution gave dark red plates of **1**. Yield: 70%. Elemental anal. Calcd for  $\text{C}_{76}\text{H}_{80}\text{Cl}_4\text{Cu}_2\text{Fe}_2\text{N}_{18}\text{O}_{18}$ : C, 47.69; H, 4.52; N, 13.17. Found: C, 47.54; H, 4.80; N, 12.68.

$[\text{Fe}^{\text{III}}_2\text{Cu}^{\text{II}}_2(\mu\text{-CN})_4(\text{dmbpy})_4(\text{imp}y)_2](\text{ClO}_4)_6 \cdot 4\text{CH}_3\text{OH} \cdot 4\text{H}_2\text{O}$  (**2**),  $[\text{Fe}^{\text{III}}(\text{CN})_2(\text{dmbpy})_2](\text{NO}_3)$  (106 mg, 0.2 mmol),  $\text{Cu}(\text{ClO}_4)_2 \cdot 6\text{H}_2\text{O}$  (74 mg, 0.2 mmol), and  $\text{imp}y$  (44 mg, 0.2 mmol) were dissolved in methanol (10 mL). To this solution was added  $(\text{Et}_4\text{N})\text{-ClO}_4$  (46 mg, 0.2 mmol) in a mixture of methanol (10 mL) and chloroform (10 mL). The resulting mixture was stored at 0 °C overnight, and bright red plates of **2** were obtained. Yield: 60%. Elemental anal. Calcd for  $\text{C}_{76}\text{H}_{84}\text{Cl}_6\text{Cu}_2\text{Fe}_2\text{N}_{18}\text{O}_{28}$ : C, 42.36; H, 4.07; N, 11.97. Found: C, 42.36; H, 3.94; N, 11.73.

**Physical Measurement.** Magnetic susceptibility data were collected in the temperature range of 2.0–300 K and in an applied field of 10 kG of a Quantum Design model MPMS SQUID magnetometer. Pascal's constants were used to determine the diamagnetic corrections.<sup>9</sup> IR spectra were obtained by using a Shimadzu FTIR 8400.

**X-ray Data Collection and Structure Refinement.** Each single crystal of **1** ( $0.05 \times 0.15 \times 0.3 \text{ mm}^3$ ) and **2** ( $0.25 \times 0.3 \times 0.3 \text{ mm}^3$ ) was mounted with epoxy resin on the tip of a glass fiber. Diffraction data were collected at  $-50$  °C on a Bruker SMART 1000 diffractometer fitted with a CCD-type area detector, and a full sphere of data was collected by using graphite-monochromated Mo  $K\alpha$  radiation ( $\lambda = 0.71073$  Å). At the end of data collection, the first 50 frames of data were re-collected to establish that the crystal had not deteriorated during the data collection. The data frames were integrated using SAINT and were merged to give a unique data set for the structure determination. Empirical absorption corrections by SADABS (G. M. Sheldrick, 1994) were carried out, and relative transmissions are 1.000–0.958 and 1.000–0.967 for **1** and **2**, respectively. Totals of 18170 ( $2^\circ < \theta < 27^\circ$ ) and 17864 ( $1.5^\circ < \theta < 23^\circ$ ) reflections were, respectively, collected for **1** and **2**, which yield 11291 ( $R_{\text{int}} = 0.0191$ ) and 6347 ( $R_{\text{int}} = 0.0549$ ) independent reflections, respectively. Information concerning the

**Table 1.** Crystal Data and Structure Refinement for  $[\text{Fe}_2\text{Cu}_2(\mu\text{-CN})_4(\text{dmbpy})_4(\text{imp}y)_2](\text{ClO}_4)_4 \cdot 4\text{CH}_3\text{OH} \cdot \text{C}_6\text{H}_6$  (**1**) and  $[\text{Fe}_2\text{Cu}_2(\mu\text{-CN})_4(\text{dmbpy})_4(\text{imp}y)_2](\text{ClO}_4)_6 \cdot 4\text{CH}_3\text{OH} \cdot 4\text{H}_2\text{O}$  (**2**)

	1	2
formula	$\text{C}_{86}\text{H}_{102}\text{Cl}_4\text{Cu}_2\text{Fe}_2\text{N}_{18}\text{O}_{22}$	$\text{C}_{80}\text{H}_{96}\text{Cl}_6\text{Cu}_2\text{Fe}_2\text{N}_{18}\text{O}_{34}$
fw	2120.44	2305.23
temp, °C	−50	−40
space group	$P\bar{1}$	$P\bar{1}$
cryst syst	triclinic	triclinic
<i>a</i> , Å	11.9749(14)	13.3088(4)
<i>b</i> , Å	13.6852(16)	14.5290(4)
<i>c</i> , Å	17.163(2)	17.1359(5)
$\alpha$ , deg	113.078(3)	69.3510(10)
$\beta$ , deg	94.366(3)	70.7150(10)
$\gamma$ , deg	92.654(4)	66.2150(10)
vol, Å <sup>3</sup>	2571.2(5)	2767.99(14)
<i>Z</i>	1	1
$\rho_{\text{calcd}}$ , Mg/m <sup>3</sup>	1.369	1.383
$\mu$ , mm <sup>−1</sup>	0.862	0.861
$\lambda$ , Å	0.71073 Å	0.71073 Å
final <i>R</i> indices <sup>a</sup>	$R1 = 0.0572$ , $[I > 2\sigma(I)]$ $wR2 = 0.1481$	$R1 = 0.0952$ , $wR2 = 0.2597$

<sup>a</sup>  $R1 = \sum ||F_o| - |F_c|| / \sum |F_o|$ .  $wR2 = [\sum [w(F_o^2 - F_c^2)^2] / \sum [w(F_o^2)^2]]^{0.5}$ . Calcd  $w = 1/[\sigma^2(F_o^2) + (0.0870P)^2 + 0.0000P]$  for **1** and  $w = 1/[\sigma^2(F_o^2) + (0.2000P)^2 + 0.0000P]$  for **2**, where  $P = (F_o^2 + 2F_c^2)/3$ .

**Table 2.** Selected Bond Lengths (Å) and Angles (deg) for  $[\text{Fe}_2\text{Cu}_2(\mu\text{-CN})_4(\text{dmbpy})_4(\text{imp}y)_2](\text{ClO}_4)_4 \cdot 4\text{CH}_3\text{OH} \cdot \text{C}_6\text{H}_6$  (**1**)<sup>a</sup>

Fe–C(2)	1.895(4)	Fe–C(1)	1.897(4)
Fe–N(4)	1.953(3)	Fe–N(6)	1.961(3)
Fe–N(5)	1.996(3)	Fe–N(3)	2.008(3)
Fe–Cu#1	4.9747(7)	Fe–Cu	4.9995(7)
Cu–N(2)	1.947(3)	Cu–N(1)	1.950(3)
Cu–N(8)	2.026(3)	Cu–N(7)	2.039(3)
Cu–O(2)	2.255(3)	N(1)–C(1)	1.158(4)
N(2)–C(2)#1	1.156(4)	O(1)–N(9)	1.281(4)
C(2)–Fe–C(1)	89.65(14)	N(2)–Cu–N(1)	92.10(12)
C(1)–N(1)–Cu	173.4(3)	C(2)#1–N(2)–Cu	171.0(3)
N(1)–C(1)–Fe	177.8(3)	N(2)#1–C(2)–Fe	176.1(3)

<sup>a</sup> Symmetry transformations used to generate equivalent atoms: #1  $-x, -y, -z$ .

crystallographic data and structure refinement are summarized in Table 1. The structures were solved by direct methods and refined by the full-matrix least-squares method on all  $F^2$  data using the SHELXTL 5.1 package (Bruker Analytical X-ray Systems). Non-hydrogen atoms were refined with anisotropic thermal parameters. Hydrogen atoms were included in calculated positions and refined with isotropic thermal parameters riding on those of the parent atoms. The relatively high *R* values for **2** were due to the low quality of the crystal and disorder of perchlorate ions and solvent molecules.

## Result and Discussions

**Description of the structures.**  $[\text{Fe}^{\text{II}}_2\text{Cu}^{\text{II}}_2(\mu\text{-CN})_4(\text{dmbpy})_4(\text{imp}y)_2](\text{ClO}_4)_4 \cdot 4\text{CH}_3\text{OH} \cdot \text{C}_6\text{H}_6$  (**1**) and  $[\text{Fe}^{\text{III}}_2\text{Cu}^{\text{II}}_2(\mu\text{-CN})_4(\text{dmbpy})_4(\text{imp}y)_2](\text{ClO}_4)_6 \cdot 4\text{CH}_3\text{OH} \cdot 4\text{H}_2\text{O}$  (**2**). Selected interatomic distances and angles for complexes **1** and **2** are listed in Tables 2 and 3, respectively; ORTEP representations are presented in Figures 1 and 2.

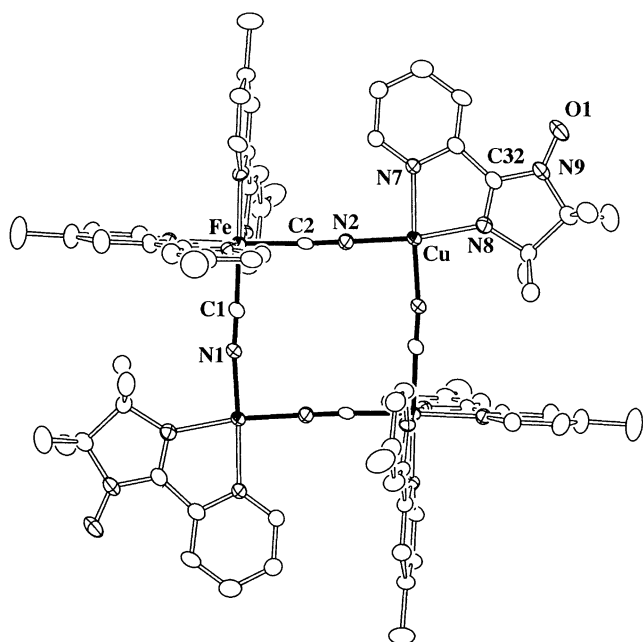
Complex cations of **1** and **2**, which locate on an inversion center, are tetranuclear macrocycles, and the overall geometry is nearly square. The square cores of **1** and **2** are, respectively, composed of the alternately cyanide bridged Fe(II) and Cu(II) ions, and Fe(III) and Cu(II) ions. The C–Fe–C and N–Cu–N bond angles of **1** are 89.3(3)° and 92.7(2)°, and those of **2** are 91.8(2)° and 88.5(1)°, respectively. The

(6) (a) Oshio, H.; Onodera, H.; Tamada, O.; Mizutani, H.; Hikichi, T.; Ito, T. *Chem. Eur. J.* **2000**, *6*, 2523. (b) Oshio, H.; Tamada, O.; Onodera, H.; Ito, T.; Ikoma, T.; Tero-Kubota, S. *Inorg. Chem.* **1999**, *38*, 5686. (c) Smith, J. A.; Galán-Mascarós, J.-R.; Clérac R.; Sun, J.-S.; Ouyang, X.; Dunbar, K. R. *Polyhedron* **2001**, *20*, 1727.  
(7) Shilt, A. A. *Inorg. Synth.* **1970**, *XII*, 248.  
(8) Shilt, A. A. *J. Am. Chem. Soc.* **1960**, *82*, 3000.  
(9) Hatfield, W. E. In *Theory and Application of Molecular Paramagnetism*; Boudreaux, E. A., Mulay, L. N., Eds.; Wiley and Sons: New York, 1976; pp 491–495.

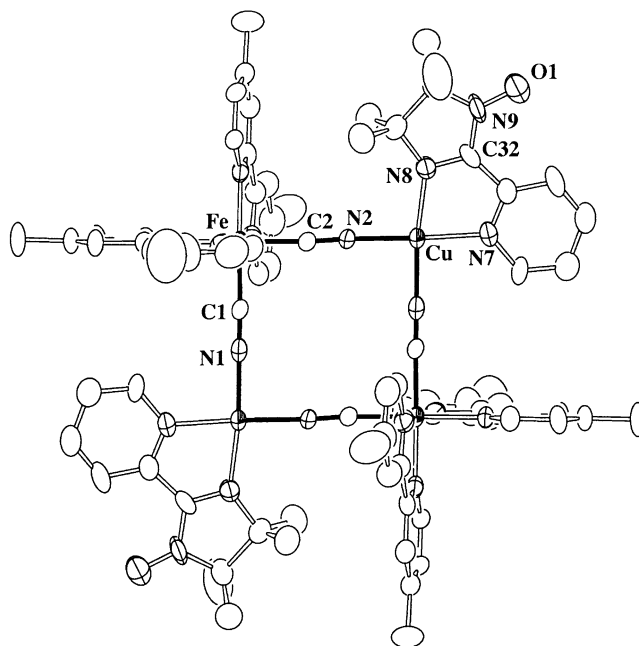
**Table 3.** Selected Bond Lengths (Å) and Angles (deg) for  $[\text{Fe}_2\text{Cu}_2(\mu\text{-CN})_4(\text{dmbpy})_4(\text{impy})_2](\text{ClO}_4)_6 \cdot 4\text{CH}_3\text{OH} \cdot 4\text{H}_2\text{O}$  (**2**)<sup>a</sup>

Fe–C(1)	1.923(11)	Fe–C(2)	1.945(10)
Fe–N(4)	1.956(8)	Fe–N(6)	1.966(8)
Fe–N(5)	1.971(6)	Fe–N(3)	1.974(7)
Fe–Cu	5.0068(16)	Fe–Cu#1	5.0368(14)
Cu–N(1)	1.958(9)	Cu–N(2)	1.974(7)
Cu–N(8)	2.015(7)	Cu–N(7)	2.027(7)
Cu–O(41)	2.230(15)	Cu–O(1S)	2.384(10)
O(1)–N(9)	1.264(10)	N(1)–C(1)	1.135(12)
N(2)–C(2)#1	1.127(11)		
C(1)–Fe–C(2)	89.2(3)	N(1)–Cu–N(2)	88.7(3)
C(1)–N(1)–Cu	172.3(10)	C(2)#1–N(2)–Cu	173.5(9)
N(1)–C(1)–Fe	178.1(9)	N(2)#1–C(2)–Fe	176.2(8)

<sup>a</sup> Symmetry transformations used to generate equivalent atoms: #1  $-x + 2, -y + 2, -z + 2$ .

**Figure 1.** Crystal structure of **1**<sup>4+</sup> (ORTEP diagram; ellipsoids at the 30% probability level). The solvent molecules coordinated to the Cu ions were omitted for clarity.

Fe...Cu edge lengths are 4.9747(7)–4.9995(5) Å for **1** and 5.007(2)–5.037(1) Å for **2**. The smaller square core of **1** was explained by the stronger  $\pi$ -back-donation from the Fe(II) ion to the cyanide groups. In **1** and **2**, the Fe(II) ions have a six-coordinate geometry with four of the coordination sites occupied by nitrogen atoms from dmbpy and the remaining cis positions occupied by the carbon atoms of the cyanide groups. The Fe–N(dmbpy) bond lengths are in the ranges 1.953(3)–2.008(3) Å for **1** and 1.956(8)–1.974(7) Å for **2**. The Fe(II)–C(CN) in **1** are shorter (1.895(3)–1.897(3) Å) than the corresponding bond lengths for the Fe(III)–C(CN) bonds in **2** (1.92(1)–1.95(1) Å), in contrast to the CN bond lengths in **1** (1.156(1)–1.158(1) Å) and **2** (1.13(1) Å). Again the shorter bond lengths can be explained by stronger  $\pi$ -back-donation in **1**. The Cu(II) ions in **1** adopt a square pyramidal geometry, in which the equatorial coordination sites are occupied by four nitrogen atoms from the bidentate impy ligand and two cyanide groups (Cu(II)–N = 1.947(3)–2.039(3) Å) and the apical position is completed by methanol (Cu–O = 2.255(3) Å). Each Cu(II) ion in **2**

**Figure 2.** Crystal structure of **2**<sup>6+</sup> (ORTEP diagram; ellipsoids at the 30% probability level). The solvent molecules coordinated to the Cu ions were omitted for clarity.

has a distorted octahedral coordination geometry with two cyanide nitrogen atoms (Cu–N = 1.958(9) and 1.974(7) Å), one impy (Cu–N = 2.015(7)–2.027(7) Å), and two solvent oxygen atoms (Cu–O = 2.23(2)–2.38(1) Å). The C–N bond distances and CN stretching frequencies of the cyanide groups for **1** and **2** are not so sensitive to the oxidation state of iron ion. The strong and weak  $\nu(\text{CN})$  bands for **1** and **2** were observed at 2119 and 2116  $\text{cm}^{-1}$ , respectively, which are in contrast to mononuclear complexes of  $[\text{Fe}(\text{CN})_2(\text{phen})_2]$  and  $[\text{Fe}(\text{CN})_2(\text{bpy})_2](\text{ClO}_4)$ . The CN bond distances in  $[\text{Fe}(\text{CN})_2(\text{phen})_2]$  and  $[\text{Fe}(\text{CN})_2(\text{bpy})_2](\text{ClO}_4)$  are 1.149(7)–1.151(7) Å and 1.123(9)–1.142(5) Å with  $\nu(\text{CN})$  bands at 2075 and 2120  $\text{cm}^{-1}$ , respectively.<sup>10</sup>

**Magnetic Properties of 1 and 2.** Temperature dependences of the magnetic susceptibilities for **1** and **2** were measured down to 2.0 K, and results are shown in Figure 3.

In **1**, the Fe(II) ions are in a diamagnetic low-spin state ( $S = 0$ ), and the Cu(II) ions and the imino nitroxide have an unpaired electron ( $S = 1/2$ ). The  $\chi_{\text{m}}T$  value of **1** did not show temperature dependence down to 10 K, and the  $\chi_{\text{m}}T$  value (2.090  $\text{emu}^{-1} \text{mol}^{-1} \text{K}$ ) at 300 K is higher than the value (1.5  $\text{emu}^{-1} \text{K mol}^{-1}$  with  $g = 2.00$ ) expected for the four uncorrelated doublets. The orthogonal arrangement of the Cu(II) magnetic orbital ( $d_{x^2-y^2}$ ) and imino nitroxide magnetic orbitals ( $p\pi^*$ ) leads to the fairly strong ferromagnetic interaction present between the Cu(II) and radical centers. Assuming that each Cu(II)–radical moiety acts as a triplet species and the two Cu(II)–radical moieties are magnetically isolated due to the low-spin Fe(II) ions, the sum of the Curie constants of the two triplets becomes 2.0  $\text{emu}^{-1} \text{mol}^{-1} \text{K}$ , which is equal to the  $\chi_{\text{m}}T$  value at 300 K. This implies that

(10) (a) Lu, T.-H.; Kao, H.-Y.; Wu, D. I.; Kong, K. C.; Cheng, C. H. *Acta Crystallogr.* **1988**, *C44*, 1184. (b) Schilt, A. A. *Inorg. Chem.* **1964**, *3*, 1323.

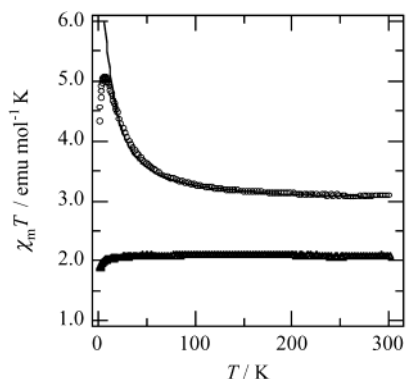


**Figure 3.**  $\chi_m T$ - $T$  plots for **1** ( $\Delta$ ) and **2** ( $\circ$ ). The solid line for **2** was calculated using the parameters given in the text.

the ferromagnetic interaction between the Cu(II) ion and the coordinated imino nitroxides is stronger than 300 K. It has been reported that the strict orthogonality of the magnetic orbitals in Cu(II)-imino nitroxide leads to the fairly strong ferromagnetic interactions ( $J > 300$  K).<sup>11</sup>

The magnetic susceptibility measurements for **2** showed a quite different behavior from **1**. The  $\chi_m T$  values for **2** increased as the temperature was lowered, and reached a maximum value of 5.065 emu mol<sup>-1</sup> K at 7.0 K. This magnetic behavior is characteristic of the occurrence of the ferromagnetic interaction in the high-temperature range. The molecular square of **2** consists of six paramagnetic centers with the Fe(III) ions in a paramagnetic low-spin state ( $S = 1/2$ ). The room temperature  $\chi_m T$  value for **2** is 3.100 emu

mol<sup>-1</sup> K, which is larger than the value (2.25 emu mol<sup>-1</sup> K for  $g = 2.0$ ) expected for the six isolated doublets. Treating the Cu(II)-radical pair as a triplet species like **1**, the  $\chi_m T$  value for the uncorrelated pair of triplets (Cu(II)-radical pair) and pair of doublets (Fe(III) ion) becomes 2.97 emu mol<sup>-1</sup> K ( $g_{\text{Fe}} = 2.15$  and  $g_{\text{Cu-radical}} = 2.05$ ). This value is in good accord with the experimental value at 300 K; the magnetic data was, therefore, analyzed using a four spin model of the two triplets (Cu(II)-radical pair) and two doublets (Fe(III) ion) with an exchange coupling constant  $J$  representing the magnetic interactions between the Fe(III) and Cu(II)-radical centers ( $H = -2J \sum S_{\text{Fe}} \cdot S_{\text{Cu-radical}}$ ). Least-squares analysis using the data above 20 K yielded the best fit values  $g_{\text{Fe}}$  and  $J$  values of 2.146(3) and 4.9(1) cm<sup>-1</sup>, respectively, where a fixed  $g_{\text{Cu-radical}}$  value of 2.050, estimated for **1**, was used. A sudden decrease of the  $\chi_m T$  values below 7 K is due to through-space antiferromagnetic interactions and/or contribution of ZFS term of the  $S = 3$  state. We also tried to analyze the magnetic data by introducing diagonal magnetic interactions, but the calculation over the whole temperature range was divergent.

In summary, the alternative arrangement of  $p\pi$ ,  $d\sigma$ , and  $d\pi$  spins in the square was a successful method for preparing a high-spin square with an  $S = 3$  spin ground state.

**Acknowledgment.** This work was partially supported by a Grant-in-Aid for Scientific Research from the Ministry of Education, Science, Sports and Culture, Japan.

**Supporting Information Available:** X-ray crystallographic files in CIF format for complexes **1** and **2**. This material is available free of charge via the Internet at <http://pubs.acs.org>.

IC0256112

(11) (a) Cogne, A.; Laugier, J.; Luneau, D.; Rey, P. *Inorg. Chem.* **2000**, *39*, 5510. (b) Luneau, D.; Rey, P.; Laugier, J.; Fries, P.; Caneschi, A.; Gatteschi, D.; Sessoli, R. *J. Am. Chem. Soc.* **1991**, *113*, 1245. (c) Oshio, H. *Inorg. Chim. Acta* **2001**, *324*, 188.